

## Article

# Influencing Factors, Risk Assessment, and Source Identification of Heavy Metals in Purple Soil in the Eastern Region of Guang'an City, Sichuan Province, China

Yuxiang Shao <sup>1</sup>, Wenbin Chen <sup>1,\*</sup>, Jian Li <sup>1</sup>, Buqing Yan <sup>1</sup>, Haiyun He <sup>2</sup> and Yunshan Zhang <sup>1</sup>

<sup>1</sup> Research Center of Applied Geology of China Geological Survey, Chengdu 610036, China; shaoyuxiangcgs@outlook.com (Y.S.); 15828188621@163.com (J.L.); 127961917@139.com (B.Y.); zhang894126621@163.com (Y.Z.)

<sup>2</sup> Eco-Environmental Sciences Research & Design Institute of Zhejiang Province, Hangzhou 310007, China; xih1210@outlook.com

\* Correspondence: 13548062965@163.com

**Abstract:** Soil heavy metal contamination poses a significant threat to both environmental health and ecological safety. To investigate the influencing factors, ecological hazards, and sources analysis of heavy metals in purple soil, 27 sets of soil samples were collected from varying genetic horizons within Guang'an City, and the contents of As, Cd, Cu, Cr, Hg, Ni, Pb, and Zn were analyzed. The results indicated higher concentrations of heavy metals in soil A horizon, compared to that of C horizon. The relevance analysis indicated that the soil's heavy metals were strongly correlated with the soil's physicochemical properties. The enrichment factor, pollution load index, and potential risk index highlighted slightly to severely polluted levels of soil Cd and Hg, which significantly contribute to the ecological hazards posed by soil heavy metals. The potential source of heavy metals analyzed using the APCS-MLR model identified both anthropogenic inputs and natural sources as primary contributors to heavy metal presence in soils. The Cu, Cr, Ni, Pb, and Zn contents in the samples from different genetic horizons were chiefly influenced by natural sources, such as soil matrix erosion and weathering, while the concentrations of Cd and Hg were largely affected by anthropogenic activities, specifically coal combustion and agriculture. Conversely, the As content was found to be influenced by a combination of both factors. Anthropogenic activities greatly impacted soil heavy metals at various depths within the study area, thereby underscoring the importance of monitoring these heavy metals. The findings gained from this research can give a scientific basis for the potential utilization of purple soil.

**Keywords:** purple soil; heavy metals; APCS-MLR; genetic horizon; source analysis



**Citation:** Shao, Y.; Chen, W.; Li, J.; Yan, B.; He, H.; Zhang, Y. Influencing Factors, Risk Assessment, and Source Identification of Heavy Metals in Purple Soil in the Eastern Region of Guang'an City, Sichuan Province, China. *Minerals* **2024**, *14*, 495. <https://doi.org/10.3390/min14050495>

Academic Editor: Anna Karczewska

Received: 18 March 2024

Revised: 28 April 2024

Accepted: 2 May 2024

Published: 7 May 2024



**Copyright:** © 2024 by the authors. Licensee MDPI, Basel, Switzerland. This article is an open access article distributed under the terms and conditions of the Creative Commons Attribution (CC BY) license (<https://creativecommons.org/licenses/by/4.0/>).

## 1. Introduction

The rise in urbanization and industrialization has significantly exacerbated soil contamination, largely due to the continuous influx of harmful substances from industries, transportation, and agriculture [1,2]. Among the various pollutants in soil, heavy metals have garnered extensive concern because of their non-degradability, high toxicity, and propensity for bioaccumulation [3,4]. High levels of heavy metals in soil not only significantly affect plant growth but also cause substantial harm to soil function, ultimately leading to a decrease in the quality and yield of food crops [5]. Moreover, heavy metals and their methyl compounds can slowly accumulate in the human body by entering through the food chain from the environment. This accumulation can cause harm to various organs, including the nervous system, kidneys, brain, and skin, thus posing a severe hazard to human health [6,7]. In 2014, the Chinese general survey of soil contamination, conducted by the Ministry of Land and Resources and China's Ministry of Environmental Protection, revealed that approximately 16.1% of the monitored soil points were polluted, with

inorganic pollutants, such as heavy metals, making up 82.8% of the total contaminated soil samples [8]. Consequently, understanding pollution levels and ecological hazards associated with soil heavy metal contamination is one of the most important prerequisites for the harmonious co-development of humans and the environment.

The accumulation of heavy metals in soil is generally associated with external factors such as exogenous inputs and soil physicochemical properties. Among them, anthropogenic inputs and natural sources are significant sources of soil heavy metals [9]. The geological input of soil heavy metals is one of the weathering products from the bedrock in the soil formation process [10]. For example, the distribution area of black shale in southwest China is abundant in metal sulfide minerals, which are easily oxidized and weathered upon exposure to the ground, resulting in elevated levels of heavy metals in the surrounding area [9,11]. In addition, human production activities, such as industrial waste disposal, fossil fuel combustion, and the use of agricultural chemicals, have considerably contributed to the issue of soil heavy metal pollution [7,12]. In recent years, practices like the irrigation of sewage water, atmospheric deposition, and the extensive use of pesticides and fertilizers have exacerbated the contamination problem in cultivated soils [13,14]. Additionally, soil physicochemical properties can impact the severity of soil heavy metal pollution. For instance, the high concentrations of cadmium and other metals in the soil of karst regions are closely associated with factors such as soil pH and mineralogical composition, typically resulting from the weathering of carbonate rocks [15]. Hence, a better understanding of the origins of these heavy metals and the physicochemical properties of the soil is vital in addressing the problem of soil heavy metal pollution.

In the past decade, multivariate statistical analysis, such as factor analysis, correlation analysis, and cluster analysis, has been commonly utilized to study the influencing factors and complex origins of soil heavy metals [16–18]. When combined with the spatial and temporal distribution of environmental media and pollutants, these analytical techniques help simplify the data and provide valuable insight into the evolving patterns of pollutants [17]. However, these methods are unable to explicitly define the contributions of various sources of soil heavy metal pollution. A series of receptor models, including positive matrix factorization (PMF), absolute principal component score multiple linear regression (APCS-MLR), the UNMIX model, the input flux model, and stable isotope tracing, were developed to quantitatively determine the source apportionment of different origins to the pollution indicators in water, sediments, or soil [19–22]. Specifically, the APCS-MLR and PMF models only require the analysis of the elemental content of various mixed sources like atmosphere, sediment, and soil. They eliminate the need for evaluating indicator content from end-member samples, such as transport emissions, industrial discharge, and agricultural fertilization [23,24]. The integrated use of multivariate statistical analysis methods and receptor models for source apportionment can enhance the identification of heavy metals in soil, contributing to the prevention of soil environmental pollution [25].

As a type of lithologic soil formed through the rapid development of purple sedimentary rocks, purple soil has highly correlated soil components and physicochemical properties with the weathering of “red beds”, which are red terrestrial clastic host rocks formed in arid and semi-arid paleoclimatic environments [26–28]. Furthermore, purple soil is often spotlighted as crucial agricultural land, especially in southwest China, leading to diverse sources of heavy metals in the soil [29,30]. In recent years, the majority of studies on heavy metals in purple soils have focused on establishing the background values [31] and baseline values [32,33]. Some scholars have conducted experimental analyses to investigate the leaching and release kinetics of heavy metals from purple soils [34], along with their adsorption by organic matter and clay minerals [35]. Several studies have compared the heavy metal concentrations in purple soil before and after intensive farming to assess the impacts of agricultural activities [36]. The results revealed that long-term intensive agricultural practices lead to a sustained increase in heavy metal concentrations in purple soil. Due to the limited fertility persistence in purple soils, it requires frequent fertilization or tilling in agricultural activities, leading to a continuous influx of heavy metals [37].

Limited research has been conducted on heavy metals in various genetic horizons of purple soil using source resolution modeling and multivariate statistical methods.

Located in the southwest of China, Guang'an City is a significant hub connecting Chengdu and Chongqing along the eastern fringe of the Sichuan Basin, renowned for its extensive purple soil areas and an abundance of resources such as coal, natural gas, and other mineral resources [38,39]. The region's steady economic development has led to consistent soil contamination from urbanization, industry, and agricultural activities. The physicochemical properties and the issue of heavy metals in purple soil have been a major concern for many scholars. To investigate the pollution status and potential sources of heavy metals in various genetic horizons of purple soil, the content of eight heavy metals (As, Cd, Cr, Cu, Ni, Hg, Pb, and Zn) were measured in the present study. The main objectives include (i) identifying the influencing factors of the heavy metal elements, (ii) evaluating the risk of heavy metal pollution in different horizons of the purple soil, and (iii) analyzing the sources of these heavy metals.

## 2. Materials and Methods

### 2.1. Study Area and Sample Collection

The study region is located in the eastern part of Guang'an City, Sichuan Province, China, encompassing the Qianfeng District, Huaying City, and Linshui County, with the location between 106°35' E–107°20' E and 30°00' N–30°40' N (Figure 1). Within the study area, there are three mountain ranges: Huaying Mountain, Tongluo Mountain, and Mingyue Mountain, extending from north to northeast, forming a unique "Three Mountains and Two Valleys" landscape [40]. Due to geological influences, the strata in the study area exhibit a zonal distribution of horizons, including the Jurassic, Triassic, Permian, and Silurian systems, as well as scattered Quaternary sediments. The Jurassic system has the largest outcrop area and consists of a series of purple-red terrestrial clastic rock formations, including siltstone, variegated mudstone, mud sandstone, and feldspathic sandstone interlaid with limestone, calcareous sandstone, and shale. The Triassic system mainly consists of the Leikoupo, Jialingjiang, Feixianguan, and Xujiuhe Formations, featuring carbonate rocks, gypsum, mudstone, and sandstone layers interspersed with coal seams. The Permian system mainly comprises the Changxing, Longtan, and Emeishan Basalt Formations, which consist predominantly of limestone interbedded with mudstone, sandstone, and basalt. The lower series of the Silurian system in this area mainly comprises purple-red mudstone and variegated mudstone layers [41].

Based on the Classification and Codes for Chinese Soil [42], the study area is characterized by four main types of soil, namely purple soil, calcareous soil, paddy soil, and yellow soil. These four soil types can be roughly classified as Cambisols, Regosols, Anthrosols, and Luvisols, following the World Reference Base for Soil Resources [43]. The purple soil, derived from purple-red terrestrial clastic rock, is prevalent in hilly terrain and primarily used for agricultural cultivation [40]. Conversely, yellow soil mainly develops on the mountain slopes within the region. Calcareous soil, found in the carbonate strata of Huaying Mountain and Tongluo Mountain, typically supports the growth of coniferous forest plants. As for paddy soil, it forms under long-term flooding conditions appropriate for rice cultivation and is mainly distributed in hilly valley areas. The major cultivated crops consist of maize, rice, and oil crops. The gardening industry is relatively well developed, with 31.67% of Guang'an City covered by forests as of 2022 [39]. Geographically, the region has a subtropical moist monsoon climate with adequate heat and precipitation and a brief frost period. The annual average precipitation and temperature in Guang'an City are approximately 1160 mm and 16 °C, respectively [39]. In addition to agriculture, the city is also abundant in mineral resources such as coal, natural gas, and rock salt. Predominantly, the coal resources are found across the fold belt areas of Huaying Mountain, Tongluo Mountain, and Mingyue Mountain [38].

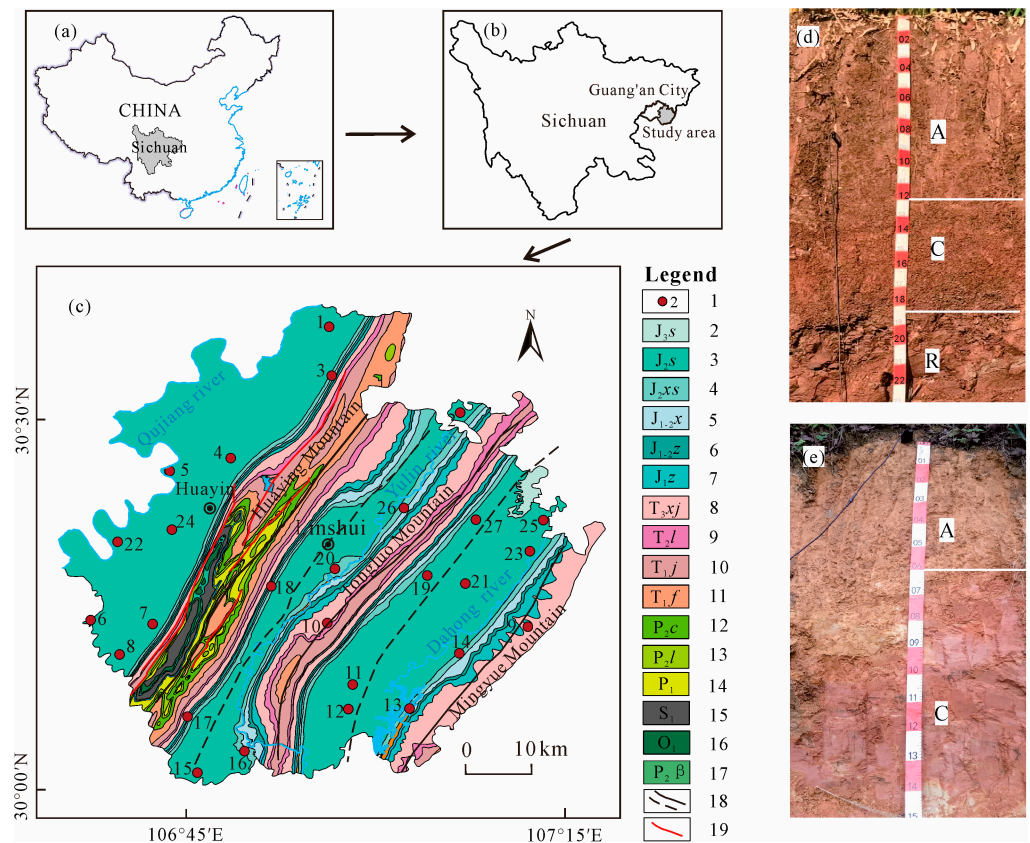


**Figure 1.** (a) The geographical position of the Sichuan Province in China; (b) a map of Guang'an City; (c) sampling and geological map; (d,e) typical purple profiles of A-C-R and A-C types. 1: Sampling sites. 2: Suining Fm. 3: Shangshaximiao Fm. 4: Xiaximiao Fm. 5: Xintiangou Fm. 6: Ziliujing Fm. 7: Zhenzhuchong Fm. 8: Xujiage Fm. 9: Leikoupo Fm. 10: Jialingjiang Fm. 11: Feixianguan Fm. 12: Changxing Fm. 13: Longtan Fm. 14: Lower Permian Series. 15: Lower Silurian Series. 16: Lower Ordovician Series. 17: Emeishan basalt. 18: Major fold axis trace. 19: Major fault (this figure is modified from the literature [40]).

In August 2022, 27 purple soil vertical profiles were investigated in the study area. The sampling sites are displayed in Figure 1c. Field survey records, including coordinates, topography, soil color, rock and mineral debris within the soil body, new soil formations (like mottles, colluvium, nodules, etc.), and other pertinent details, were compiled in accordance with the technical specifications outlined in the Field Soil Description and Sampling Manual [44]. Soil profile sites were generally selected in cultivated drylands where the soil types could be easily identified, and the terrain was relatively uniform. According to the soil occurrence characteristics [42], the collected soil profiles are generally stratified into A, C, and R horizons from the top layer downwards, and few collected profiles have a B horizon (Figure 1d,e). To prevent cross-contamination, each soil or rock sample from the occurrence layer was collected approximately 2 kg from bottom to top. The collected samples comprised 27 surface soil samples (A horizon), 27 matric soil samples (C horizon), and 10 bedrock samples (R horizon). The A horizon typically ranges in depth from 0 to 30 cm, characterized by a loose soil structure, abundant plant roots, and high humus content. The C horizon typically ranges in depth from 30 to 80 cm, with a few coarse roots and sporadic bedding structures. The bedrock horizon (R horizon), composed of interbedded purple-red sandstone and mudstone, is located below 80 cm (and sometimes less than 80 cm).

## 2.2. Sample Preparation and Analysis

The collected samples were stored in well-ventilated warehouses for natural air-drying. Any impurities within the samples, such as roots, plant and animal debris, and gravel,

were removed to prevent contamination. To further ensure that the processing was free of contamination, the sample processing sites were selected in rural areas, distant from highways and urban areas. The air-dried samples were crushed using a wooden stick or rubber mallet and sieved through a 2 mm sieve. The unsifted soil particles needed to be crushed again and sieved repeatedly until all samples could pass through the 2 mm sieve. The processed soil samples were then stored in appropriately labeled plastic bags and sent to the laboratory for further analysis.

After the samples were sent to the laboratory, a small portion of soil was initially extracted for testing the pH and texture. Soil pH was determined using the glass electrode method. Soil texture was analyzed using a laser particle size analyzer (AS200, Retsch, Haan, Germany), and the corresponding masses were measured with an accuracy of 0.1 mg. About 100 g of the remaining sample was ground using an agate mortar and sieved through a 0.15 mm nylon sieve for subsequent testing. Each soil sample was initially digested with a tetra-acid solution of HCl, HNO<sub>3</sub>, HClO<sub>4</sub>, and HF, and then transferred to volumetric flasks [45]. The concentrations of Hg and As in the soil samples were determined using an atomic fluorescence spectrophotometer (AFS-230E, Beijing Haiguang Instrument Co., Beijing, China). The levels of Cd, Ni, Cr, Cu, Pb, Zn, Al, and Fe were analyzed using an inductively coupled plasma mass spectrometer (ICP-MS-iCAP6300, Thermo Fisher Scientific, Waltham, MA, USA). Blank samples and national first-level standard substances (GSS-17, GSS-19, GSS-28) [46] were mixed in the processes of sample testing to ensure the accuracy of the experimental data. No blank samples were detected in the analysis procedure. The measurement errors of the elements from the standard substances ranged from 1.22% to 8.35%, meeting the quality requirements [45]. All samples were determined at the Southwest China Supervision and Inspection Center of Mineral Resources, Ministry of Land and Resources.

### 2.3. Data Processing Methods

#### 2.3.1. Enrichment Factor

The enrichment factor (EF) is a significant index commonly utilized to assess the pollution levels of toxic components in river sediments, soils, and substrates [47]. This method takes into account both the natural origins and the human pollution factors and intuitively displays the level of pollution [48]. It is calculated according to this formula:

$$EF = \frac{(C_i / C_{re})_{\text{sample}}}{(C_i / C_{re})_{\text{background}}} \tag{1}$$

where  $C_i$  and  $C_{re}$  represent the test concentration or background value of soil component  $i$  and the reference component. The reference elements should be chemically stable, abundant, and minimally affected by human activities, such as Zr, Mn, Al, and Sc [49]. The composition of soil elements in purple soil differs significantly from that in other soil types. Therefore, the average values of elements in Chinese purple soils, derived from a comprehensive collection of diverse soil profiles, along with standardized testing and meticulous data analysis spearheaded by the State Environmental Protection Bureau of China in 1990, were utilized as the background values in this research [31]. The pollution levels and their corresponding interval values are shown in Table 1.

**Table 1.** Pollution levels of enrichment factor, pollution load index, and potential ecological risk index.

EF	Pollution Level	CF, PLI	Pollution Level	E <sub>r</sub> <sup>1</sup>	Pollution Level	I <sub>RI</sub>	Pollution Level
<1	Uncontaminated	<1	Uncontaminated	<40	Low	<150	Low
1~2	Light	1~2	Moderate	40~80	Moderate	150~300	Moderate
2~5	Moderate	2~3	Heavy	80~160	Considerable	300~600	High
5~20	Heavy	>3	Extreme contaminated	160~320	High	>600	Very high
20~40	Severe	-	-	>320	Very high	-	-
>40	Very heavy	-	-	-	-	-	-

### 2.3.2. Pollution Load Index

This method is used to evaluate the cumulative heavy metal contamination at a sample location or across a broader region [50]. The calculations for this assessment are as follows:

$$CF_{ij} = C_{ij}/S_i \quad (2)$$

$$PLI_j = \sqrt[n]{CF_{1j} \times CF_{2j} \times \dots \times CF_{nj}} \quad (3)$$

where  $CF_{ij}$  represents the contamination factor for the soil component  $i$ .  $C_{ij}$  stands for the tested concentration of component  $i$ , while  $S_i$  represents the background value of component  $i$ .  $PLI_j$  is the cumulative loading index in sample  $j$ , and  $n$  represents the number of heavy metals involved in the assessment. The calculation results of PLI and the corresponding pollution levels are shown in Table 1.

### 2.3.3. Potential Ecological Risks

The evaluation method for potential ecological risks incorporates factors such as the toxicity level, the background value, and the combined effect of multiple elements [51]. The calculations are stated below:

$$E_r^i = T_r^i \times C_i/S_i \quad (4)$$

$$I_{RI} = \sum_{i=1}^n E_r^i \quad (5)$$

where  $E_r^i$  represents the potential hazard factor of element  $i$ .  $C_i$  represents the measured concentration of element  $i$ .  $S_i$  is the geochemical background value of element  $i$ .  $I_{RI}$  is the complete potential ecological risk of a site.  $n$  is the number of different heavy metal species at the sampling site.  $T_r^i$  represents the heavy metal toxicity response value, which was as follows in descending order: Hg (40), Cd (30), As (10), Cr (5), Ni (5), Pb (5), Cu (2), and Zn (1) [52]. The classifications of  $E_r^i$  and  $I_{RI}$  are presented in Table 1.

### 2.3.4. APCS-MLR Model for Source Analysis

By integrating the principal component scores derived from factor analysis into multiple linear regression, the APCS-MLR method quantitatively delineates the contribution of various pollution sources to elements within the polluted environment [19]. Furthermore, factor analysis serves as a statistical technique for simplifying a dataset by creating new variables that capture the important information from the original variables, ultimately reducing the complexity of the data [53]. In this study, this analytical approach was employed to identify the origins and influencing factors of soil heavy metal contamination. Prior to conducting factor analysis, it is essential to first perform the Bartlett's sphericity and Kaiser–Meyer–Olkin tests to evaluate the suitability of the dataset. Eigenvalues and eigenvectors were obtained by performing variance rotation through a linear combination of eigenvectors and original variables. Subsequently, principal components with eigenvalues above 1 were selected to capture the most meaningful information about the variables. Based on the principal components, the potential sources of soil heavy metals were investigated.

The fundamental principle of the APCS-MLR model involves performing multiple linear regression using the normalized scores obtained from factor analysis. The resulting regression coefficients are then utilized to determine the contribution of each factor associated with the pollutant source. Negative values may arise during the calculation process, potentially compromising the accuracy of pollutant source analysis. The contribution of pollution sources to heavy metal elements can be calculated using the absolute values of negative figures [23,25]. The formula is as follows:

$$C_i = b_{0i} + \sum_1^p (b_{pi} + APCS_p) \quad (6)$$

where  $C_i$  represents the heavy metal concentration.  $b_{0i}$  and  $b_{pi}$  are the constants and coefficients in the multivariate linear regression.  $APCS_p$  is the absolute score of the principal component. The average value of  $b_{pi} \times APCS_p$  stands for the contribution of the source to the particular heavy metal.

### 3. Results and Discussion

#### 3.1. Physicochemical Properties of the Purple Soil

In this research, the pH levels of the purple soil A horizon varied from 4.29 to 7.84, with an average of 5.95. Similarly, the pH levels in the soil C horizon varied from 4.86 to 7.59, with an average value of 6.03. Only a small number of soil samples had a pH greater than 7, indicating the slightly acidic nature of the purple soil (Table 2). The pH of soil is an important indicator that affects the geochemical activities of heavy metals. Soil acidification significantly impacts the toxicity, adsorption capacity, bioavailability, and accumulation of heavy metals [54]. It has been evidenced from related studies that long-term intensive farming, the use of nitrogen fertilizer, and the loss of base cations during soil erosion are important causes of soil acidification in purple soils [29]. Al and Fe are the primary constituents of soil, and their oxides play an important role in stabilizing soil structure [55]. The A and C horizons exhibited average concentrations of  $Al_2O_3$  at 15.9% and 16.3%, respectively. In comparison, the total Fe concentrations within the same horizons averaged 5.2% and 5.1%, respectively. Both of them are slightly higher than their respective background values of the Chinese purple soil [31].

**Table 2.** Physicochemical properties and heavy metals concentrations of the soil profile in the study area.

Parameters		Sand	Silt	Clay	pH	$Al_2O_3$	$TFe_2O_3$	As	Cd	Cr	Ni	Cu	Hg	Pb	Zn
A horizon	Min	18.8	9.3	3.3	4.29	13.6	2.6	1.61	0.06	39.0	12.0	5.0	0.016	15.4	25.6
	Max	83.6	46.8	40.1	7.84	21.2	7.7	8.53	0.35	91.2	49.1	33.5	0.082	37.6	99.2
	Avg	47.4	29.9	22.7	5.95	15.9	5.2	4.45	0.17	65.1	29.4	22.7	0.042	25.5	76.1
	SD	16.0	9.6	7.6	0.92	1.6	1.0	1.70	0.08	11.1	7.3	6.3	0.017	4.4	16.3
	CV	0.35	0.34	0.36	0.16	0.10	0.20	0.38	0.45	0.17	0.25	0.28	0.41	0.17	0.21
C horizon	Min	25.3	8.5	4.8	4.86	13.4	1.8	0.97	0.05	37.9	14.2	6.3	0.006	17.5	25.7
	Max	86.2	47.9	34.3	7.59	21.0	9.0	13.10	1.38	98.9	50.5	40.0	0.178	39.4	95.4
	Avg	57.3	26.4	16.3	6.03	16.3	5.1	3.68	0.16	64.8	30.0	21.7	0.029	24.6	73.3
	SD	18.5	11.4	8.6	0.80	1.5	1.4	2.58	0.24	14.5	8.7	7.8	0.032	5.1	20.0
	CV	0.32	0.43	0.52	0.13	0.09	0.28	0.70	1.57	0.22	0.29	0.36	1.11	0.21	0.27
R horizon	Min	-	-	-	-	11.0	2.8	1.33	0.05	54.8	23.4	17.3	0.013	16.6	62.4
	Max	-	-	-	-	17.7	7.7	16.20	0.17	88.8	59.0	55.5	0.076	38.5	107.0
	Avg	-	-	-	-	15.5	5.9	5.31	0.12	70.9	37.9	30.4	0.026	25.0	91.3
	SD	-	-	-	-	1.7	1.4	4.44	0.04	8.3	9.1	10.0	0.017	5.9	14.6
	CV	-	-	-	-	0.11	0.23	0.84	0.36	0.12	0.24	0.33	0.66	0.24	0.16
Background values of the Chinese purple soil [31]	-	-	-	-	-	13.8	4.9	8.4	0.0752	60.6	28.1	24.6	0.0326	25.8	77.5
Continental crustal background [56]	-	-	-	-	-	28.8	4.3	1.7	0.1	126	56	25	0.04	14.8	65

Notes: The annotation  $TFe_2O_3$  denotes the cumulative iron content present within the analyzed soil sample, reported in the form of  $Fe_2O_3$ . The unit for heavy metal,  $Al_2O_3$ , and  $TFe_2O_3$  concentrations is mg/kg. The unit for sand, silt, and clay is %. The pH value is dimensionless.

Based on the international soil texture classification [57], the soil in the study area was primarily classified as loam or sandy loam (Figure 2). In the soil's A horizon, the sand, silt, and clay contents varied from 18.8% to 83.6%, 9.3% to 46.8%, and 3.3% to 40.1%, with average values of 47.4%, 29.9%, and 22.7%, respectively. Meanwhile, in the soil's C horizon, the quantities of sand, silt, and clay ranged from 25.3% to 86.2%, 8.5% to 47.9%, and 4.8% to 34.3%, with average values of 57.3%, 26.4%, and 16.3%, respectively. The A horizon displayed a higher composition of clay or silt and a lower composition of sand compared to the C horizon, inconsistent with the typical results of soil sedimentation processes. This irregularity may be ascribed to the weathering of the purple soil from red beds of sandstone and mudstone interbedded with a relatively short period of soil formation, without any apparent mechanical depositional processes [58].

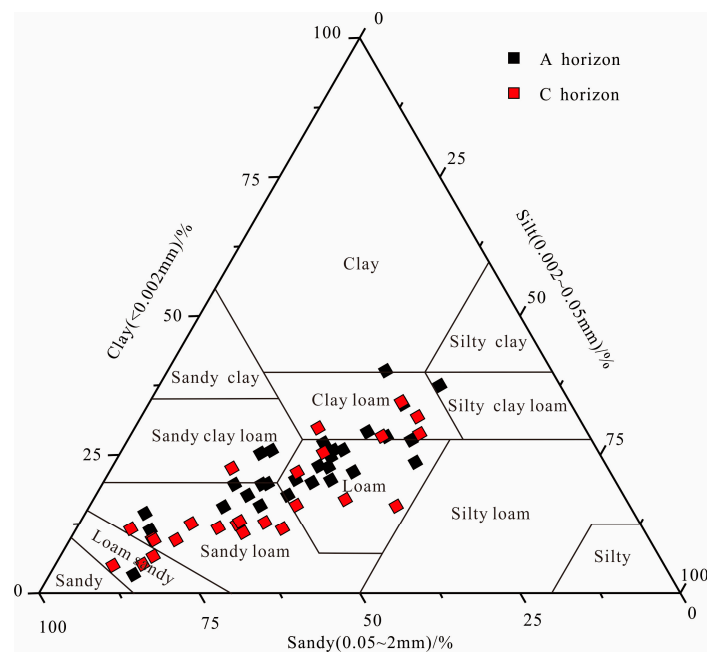


**Figure 2.** Triangle coordinates of the soil texture classification in the different soil horizons.

### 3.2. The Contents of Heavy Metals and Correlation Analysis

Descriptive statistics of heavy metals from different soil horizons are shown in Table 2. Compared to the continental crustal background [56], the heavy metals such as Cr (70.9 mg/kg), Ni (37.9 mg/kg), and Hg (0.026 mg/kg) in the parent rocks of this study area were relatively depleted. Conversely, Cd (0.12 mg/kg), Cu (30.4 mg/kg), Zn (91.3 mg/kg), Pb (25.0 mg/kg), and As (5.31 mg/kg) were mildly enriched. The concentrations of heavy metals in the A and C horizons of the purple soil in this research were similar to those in the parent rock. The average concentrations in the topsoil (A horizon) decreased in the following order: Zn (76.1 mg/kg) > Cr (65.1 mg/kg) > Ni (29.4 mg/kg) > Pb (25.5 mg/kg) > Cu (22.7 mg/kg) > As (4.45 mg/kg) > Cd (0.17 mg/kg) > Hg (0.042 mg/kg). Compared with the background values of the Chinese purple soil [31], the levels of Cd, Cr, Ni, and Hg in the A and C horizons were considerably enriched, with Cd displaying a magnitude of enrichment. On the other hand, the concentrations of Zn, Pb, As, and Cu were all lower than the background values [31]. Statistically, the concentrations of heavy metals in the A horizon exceeded the Chinese purple soil background values in the following order: Cd (89%) > Hg (67%) > Ni (63%) = Cr (63%) > Zn (59%) > Pb (44%) > Cu (41%) > As (4%). Similarly, in the C horizon, the concentrations followed this sequence: Cd (74%) > Ni (63%) = Cr (63%) > Zn (52%) > Cu (37%) > Pb (33%) > Hg (19%) > As (4%).

Figure 3 shows the relationships among the soil texture, pH levels, and the concentration of heavy metals in the local soils. The correlation analysis displayed significantly positive correlations among metals, such as As, Zn, Cr, Ni, Pb, and Cu, implying similar geochemical properties or the same origins. Hg and Cd in the soils exhibited distinct patterns of correlation when compared with other heavy metals. In the different soil horizons, soil Hg did not show a significant correlation with the majority of other heavy metals, as most of the absolute values of the correlation coefficients were below 0.3. On the contrary, the correlation coefficients between soil Cd and other heavy metals ranged from 0.069 to 0.572. Only Ni, Cu, and Zn in C horizons had correlation coefficients with Cd above 0.4. The findings indicated that the soil Hg and Cd might have different geochemical properties from other heavy metals in the local soils.

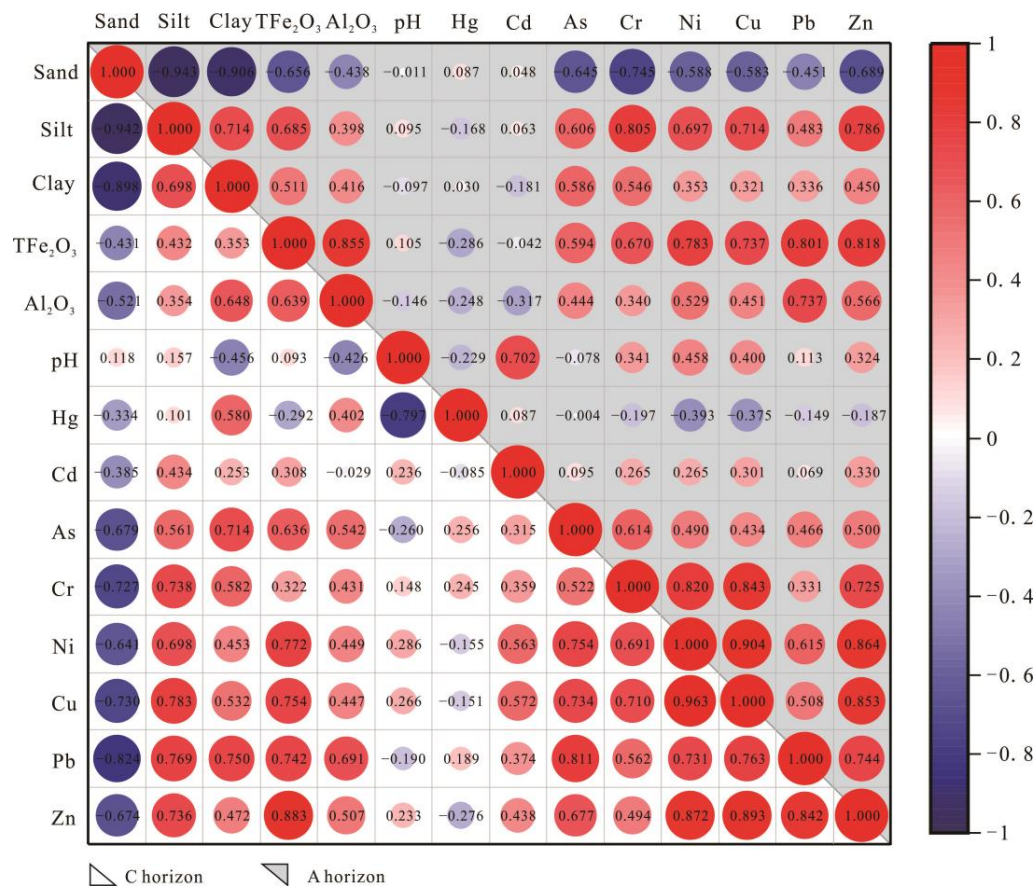


**Figure 3.** Correlation between the heavy metal contents and physicochemical properties of the soil samples.

The heavy metals, except for Cd and Hg, showed a positive correlation with the concentrations of soil silt, clay, Fe, and Al, and a negative correlation with the soil sand content. The results suggested that heavy metals, such as As, Zn, Cr, Ni, Pb, and Cu, were easily adsorbed by fines, clay particles, or Fe- and Al-containing minerals. Soil texture and major components were significant factors affecting the concentration of heavy metals in soil [15]. However, Cd or Hg in the soil exhibited a relatively significant correlation with silt, clay, and Al<sub>2</sub>O<sub>3</sub> only in the C horizon, which may indicate artificial input or mixed sources for these elements. In the soil horizons A and C, the correlation coefficients between Hg and pH were -0.229 and -0.797, respectively. In contrast, Cd displayed a positive correlation with pH, with correlation coefficients displaying 0.702 and 0.236 in soil horizons A and C, respectively. Other heavy metal elements showed weak to moderate positive correlations with soil pH, with correlation coefficients ranging from 0.148 to 0.458. An increase in soil pH typically enhances the negative charges on the surfaces of clay minerals and organic matter, encouraging a transition in electrostatic absorption towards specialized absorption. The latter absorption boasts stronger binding forces, resulting in the accumulation of heavy metals in the soil [5]. However, the geochemical behavior of Hg in soil is relatively complex. Several studies have shown that increased pH levels lead to the formation of Hg(OH)<sub>x</sub><sup>(2-x)</sup> hydroxyl complexes with soil OH, thereby enhancing mercury mobility and introducing a negative correlation between soil Hg and pH [59].

### 3.3. Evaluation of Heavy Metal Contamination in the Purple Soil

#### 3.3.1. Evaluation of EF

In this study, the concentration of Al<sub>2</sub>O<sub>3</sub> was abundant and consistently distributed in the soil, exhibiting a variation coefficient of less than 0.10 (Table 2). Therefore, Al<sub>2</sub>O<sub>3</sub> was

chosen to be the reference component. Based on the pollution levels of EF (Table 1), most of the heavy metals exhibited point pollution in various horizons, except for Cd and Hg, which showed mild or heavy pollution (Figure 4). In the soil samples, the uncontaminated, slightly contaminated, and moderately contaminated states accounted for 26%, 26%, and 48% of the total samples, respectively. The Hg level had 33% of the collected samples in a lightly contaminated state, and 67% of them in an uncontaminated condition. Other heavy metals were found in an uncontaminated state, with the average EF values in the order of Cr (0.8)  $\approx$  Ni (0.8) > Pb (0.7)  $\approx$  Zn (0.7)  $\approx$  Cu (0.7) > As (0.4).

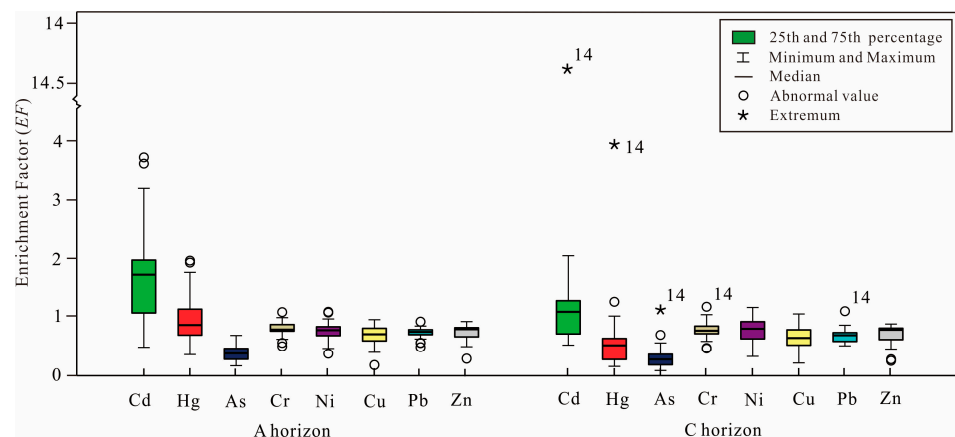


**Figure 4.** The enrichment factor (EF) for the soil heavy metals in the study area.

Similarly, the concentrations of As, Cr, Cu, Ni, Pb, and Zn in the C horizon were in an uncontaminated state, with the average EF values of 0.8, 0.8, 0.6, 0.7, 0.6, and 0.3, respectively. For the Cd concentration in the C horizon, one sample was heavily polluted, one sample was moderately polluted, 44% of the samples were lightly contaminated, and 48% were uncontaminated. For the Hg concentration in the C horizon, 11% was under conditions of moderate to slight pollution, while the remaining percentage was uncontaminated. The high EF values of Hg and Cd in the investigated soils, especially in the top soils, may be related to the development of metallic mineral resources and agricultural activities [60,61]. In addition, other heavy metals with EF less than 1 suggest that the pure migration of these elements in the area might have occurred during rock weathering and soil formation. An extremum in the C horizon, showing moderate or heavy contamination, may be related to the presence of ferromanganese nodules within it [59].

### 3.3.2. Evaluation of PLI

The average CF values of the various heavy metals in the A horizon were ranked in the following descending order: Cd > Hg  $\approx$  Cr  $\approx$  Ni > Pb  $\approx$  Zn  $\approx$  Cu > As, with the respective means of 2, 1, 1, 1, 0.9, 0.9, 0.9, and 0.5 (Table 3). In the C horizon, the average CF values were as follows: Cd (2), Cr (1), Ni (1), Pb (0.9), Zn (0.9), Hg (0.9), Cu (0.9), and As (0.4) (Table 3). The CF values for As, Cr, Cu, Ni, Pb, and Zn in the soils were either equal to or less than 1, indicating minimal ecological risk from these metals in this study. The CF values for Hg and Cd in most soil samples were greater than 1, suggesting moderate to heavy pollution levels. Based on pollution risk levels for PLI (Table 1), the majority of the soil samples exhibited a moderate level of contamination (Table 3, Figure 5). The PLI values of the A horizon ranged from 0.6 to 1, with 59.3% of the samples exceeding 1. In contrast, the PLI values of the C horizon varied from 0.5 to 2. Among them, one sample exceeded 2, and 22.2% of the total samples from the C horizon represented moderate contamination. The results indicated that surface soil samples showcased more instances of moderate–heavy metal contamination compared to their deeper counterparts. However, Cd and Hg emerged as the predominant heavy metal pollutants in the soils of the investigated area.

**Table 3.** Evaluation results of pollution load index and potential ecological risk index of heavy metals in the soil genetic horizons from the study area.

Genetic Horizons	Pollution Load Index									Potential Ecological Risk Index									
	CF <sub>As</sub>	CF <sub>Cd</sub>	CF <sub>Cr</sub>	CF <sub>Ni</sub>	CF <sub>Cu</sub>	CF <sub>Hg</sub>	CF <sub>Pb</sub>	CF <sub>Zn</sub>	PLI	E <sub>r</sub> <sup>As</sup>	E <sub>r</sub> <sup>Cd</sup>	E <sub>r</sub> <sup>Cr</sup>	E <sub>r</sub> <sup>Ni</sup>	E <sub>r</sub> <sup>Cu</sup>	E <sub>r</sub> <sup>Hg</sup>	E <sub>r</sub> <sup>Pb</sup>	E <sub>r</sub> <sup>Zn</sup>	I <sub>RI</sub>	
A horizon	Min	0.2	0.8	0.6	0.4	0.2	0.5	0.6	0.3	0.6	2	23	3	2	0.4	20	3	0.3	71
	Max	1	5	2	2	1	3	1	1	1	10	139	8	9	3	101	7	1	249
	Avg	0.5	2	1	1	0.9	1	0.9	0.9	1	5	69	5	5	2	51	5	1	143
C horizon	Min	0.1	0.6	0.6	0.5	0.3	0.2	0.7	0.3	0.5	1	19	3	3	0.5	7	3	0.3	57
	Max	2	18	2	2	2	5	2	1	2	16	551	8	9	3	218	8	1	809
	Avg	0.4	2	1	1	0.9	0.9	0.9	0.9	0.9	4	62	5	5	2	35	5	1	120

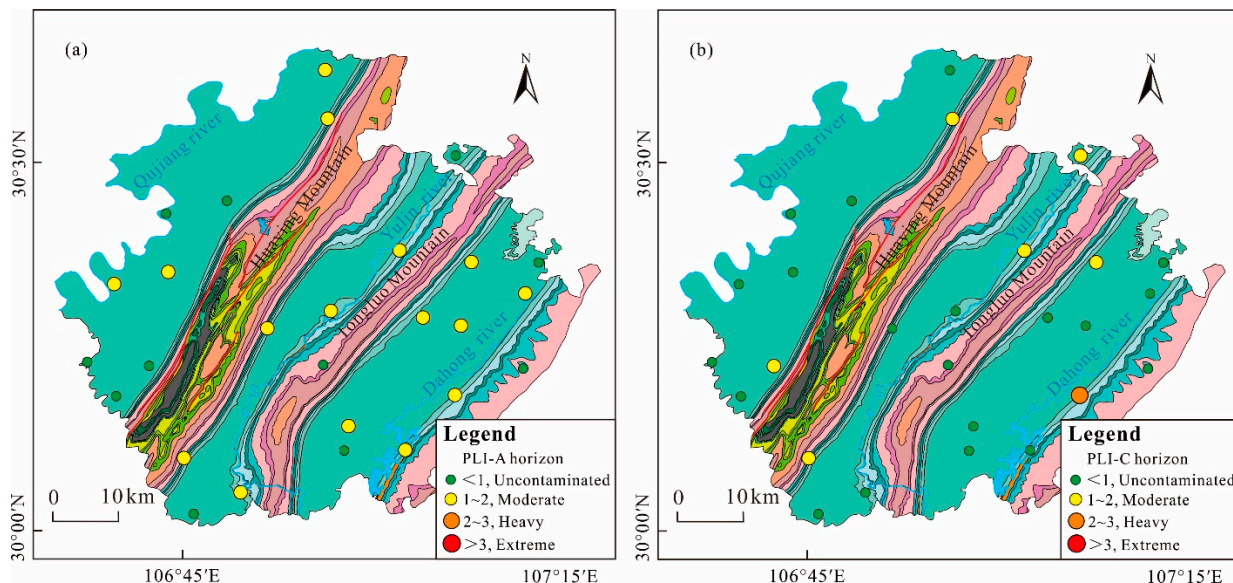


**Figure 5.** Scatter plot of soil heavy metal PLI evaluation in the study area: (a) in A horizon; (b) in C horizon. (The stratigraphic legend is consistent with Figure 1).

### 3.3.3. Evaluation Results of Potential Ecological Risk

The  $E_r^i$  and  $I_{RI}$ , which represent the potential ecological hazard posed by each individual heavy metal and each soil sample, are summarized in Table 3 and Figure 6. According to the  $E_r^i$  values, the concentrations of As, Cu, Cr, Ni, Pb, and Zn showed no potential ecological risks in the A and C horizons of the purple soil. However, the Cd and Hg levels in the soil ranged from low to moderate potential ecological hazards. In the C horizon, the percentages of low, moderate, and high pollution ecological hazards related to Cd were 41%, 7%, and 4%, respectively. As for Hg, the percentages for low and moderate contamination ecological hazards were 15% and 4%. In the A horizon, the low and moderate pollution ecological hazards for Cd accounted for 52% and 22% of the samples, while the proportions for low and moderate pollution ecological hazards for Hg were 52% and 15%. The potential ecological hazards of Hg and Cd in the topsoil of the study area were relatively higher than those in the deep soil.

The  $I_{RI}$  values of the topsoil in this study varied from 71 to 249, with 33% of the samples exceeding 150, indicating that the soils were moderately hazardous with localized ecological risk (Figure 6). However, the  $I_{RI}$  values of the soil parent material layer ranged from 57 to 809, with only a single sample exceeding 150 (Figure 6). The findings indicated that the deep soils in this region were less hazardous than the topsoil. A comprehensive analysis showed that Hg and Cd concentrations, which may be affected by agricultural or atmospheric inputs, were the main contaminants in the purple soil of the study region. According to the risk assessments of the EF, CF, and  $E_r^i$  in the soils (Table 3), the concentrations of As, Cu, Cr, Ni, Pb, and Zn in the samples were found to be in an uncontaminated condition and categorized as low ecological hazards. However, due to their higher contents and

toxicity response factors, Hg and Cd within the soil were categorized as medium ecological hazards. Considering the difference in soil texture in the purple soil horizons, along with the significant correlation between soil texture and various heavy metal concentrations, the high EF, CF, and  $E_r^1$  values may not solely result from actual pollution but could also be affected by assuming undifferentiated background values for all purple soils.

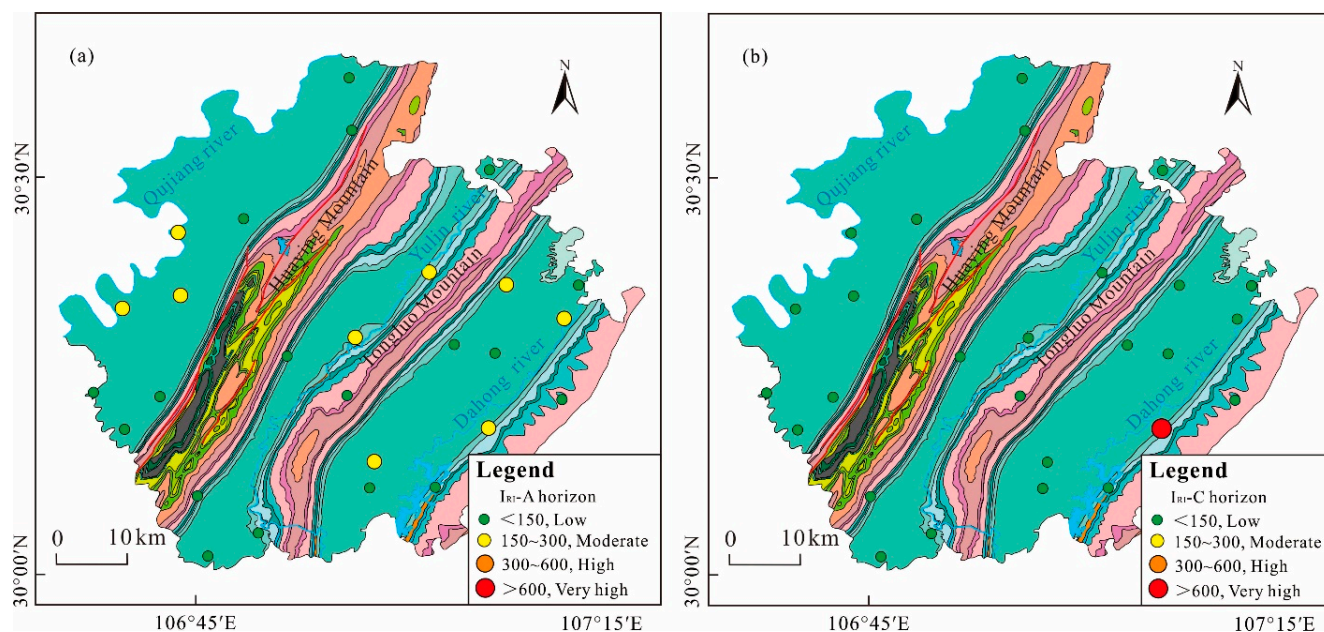


**Figure 6.** Scatter plot of soil heavy metal  $I_{RI}$  evaluation in the study area: (a) in A horizon; (b) in C horizon. (The stratigraphic legend is consistent with Figure 1).

### 3.4. Heavy Metal Source Analysis

#### 3.4.1. PCA Analysis

A factor analysis was employed to have a clear understanding of the origins of soil heavy metals in the study region (Figure 7a,b). Before conducting the factor analysis, the soil element contents successfully passed the Kaiser–Meyer–Olkin (KMO) measurement test with a value of 0.809 and Bartlett’s sphericity test at a significance level of  $p < 0.05$  [17]. These results indicated that the elements were highly correlated and appropriate for principal component analysis. After the varimax orthogonal rotation of Kaiser standardized data, two main component factors were identified with initial eigenvalues exceeding 1. The two main principal components (PCs) contributed 50.53% and 27.77% of contributions, respectively, with a cumulative contribution rate of 78.30% (Table 4), explaining the majority of information on soil heavy metals in the research area. The elements Cr, Cu, Ni, and Zn have strong loadings ( $>0.75$ ) on PC1, while Pb and As have medium loadings (0.5–0.75) on PC1 (Table 4, Figure 7a). The contents of these elements had a strong positive correlation with each other, indicating a possible shared origin. The heavy metals with high loadings in PC1 mostly had enrichment factors (EFs) less than 1, suggesting that natural factors, including the erosion and weathering of the matrices, were primarily responsible for contributing to PC1.

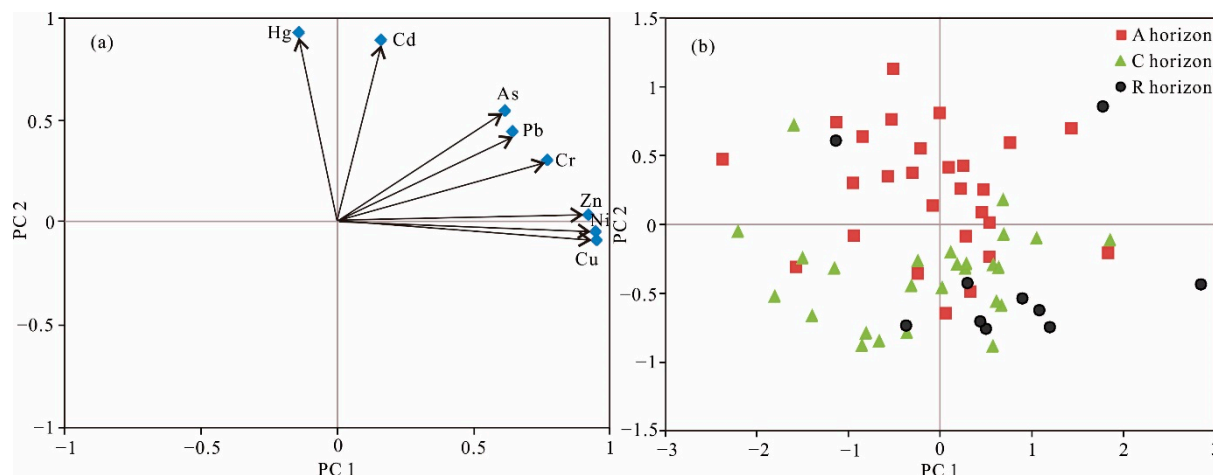


**Figure 7.** Principal component analysis of heavy metals in the samples from the study area: (a) loading plot of the elements; (b) score plot of each sample.

**Table 4.** Loadings of each heavy metal, eigenvalues, and variance in the PCA analysis.

Heavy Metals	Ni	Cu	Zn	Cr	Pb	As	Hg	Cd	Eigenvalues	Variance (%)
PC1	0.947	0.944	0.917	0.767	0.639	0.611	−0.143	0.158	4.308	50.53
PC2	−0.091	−0.049	0.032	0.300	0.439	0.540	0.923	0.886	1.955	27.77

The contents of Hg and Cd had relatively high loadings (0.886~0.923) in PC2, while As content had a medium loading (0.540) (Figure 7a). The heavy metal Hg has the characteristics of low viscosity and high mobility, and is one of the few volatile heavy metals, making it easy to enter the atmospheric cycle [60]. Particularly, Hg is an important pollutant produced by coal combustion and can be easily deposited into the atmosphere at high temperatures, consequently leading to topsoil contamination [12]. The Huaying Mountains in the study area are rich in coal resources, leading to the accumulation of heavy metals such as Hg, Cd, and Zn in the surrounding soils due to coal mining and utilization. Therefore, coal combustion may be a primary contributor to PC2. Although coal contains abundant amounts of Cd, soil Cd sources are more diverse, encompassing mining, metallurgy, pesticides, and fertilizers [36]. The limited association between Hg and Cd in the soil indicated that these two elements might not originate from similar sources (Figure 3). Prevailing research has shown a considerable enrichment of soil Cd and As under high-intensity farming conditions [36,41]. Meanwhile, the study area has little mining activity of cadmium sulfide-containing ores, such as sphalerite and desclozite [39]. Therefore, the soil Cd predominantly originated from anthropogenic inputs, including chemical fertilizers and pesticides used in farming. A comprehensive analysis of the above reveals that PC2 may be jointly affected by a blend of human-induced sources, such as atmospherically transported coal and agricultural activities.

The loadings of the sample points in the PCA figure (Figure 7b) displayed that the soil samples from the A horizon were closer to PC2. Conversely, the soil samples from the parent rock horizon (R horizon) exhibited more proximity to PC1. This pattern further indicated anthropogenic sources of heavy metals, including Cd and Hg, were primarily occurring in the topsoil of the study area.

### 3.4.2. APCS-MLR Source Analysis

According to the contamination sources obtained via the PCA analysis, the principal component fraction multiple linear regression model was used to estimate the contribution of pollution sources to the heavy metals in various soil horizons. The fitting degree and reliability of the APCS-MLR analysis were discussed by evaluating the adjusted R-squared

value and the ratio of measured to predicted average concentrations of elements [24,61]. The results are displayed in Table 5. The ratios of measured and predicted data were close to 1. Furthermore, the fitted R-squared values for the remaining heavy metals were mostly above 0.7, except for As (0.414), Cd (0.437), and Pb (0.432) in the topsoil (A horizon). These findings indicated that the APCS-MLR method demonstrated a high degree of fit.

**Table 5.** Sources contributions and fitting degrees of APCS-MLR model.

Heavy Metals		As	Cd	Hg	Pb	Cr	Ni	Cu	Zn
A horizon	PC1 contribution (%)	81.1	41.4	22.0	38.8	49.1	69.5	76.7	66.6
	PC2 contribution (%)	18.8	50.3	57.8	1.6	2.9	6.0	5.3	3.7
	Unexplained variability (%)	0.1	8.3	20.2	59.6	48.0	24.5	18.0	29.7
	Measured mean (mg/kg)	4.45	0.17	0.042	25.5	65.1	29.4	22.7	76.1
	Predicted mean (mg/kg)	4.45	0.17	0.030	25.5	65.1	29.4	22.7	76.1
	R <sup>2</sup>	0.41	0.44	0.76	0.43	0.73	0.91	0.86	0.86
C horizon	PC1 contribution (%)	59.0	20.1	14.1	36.5	42.2	85.4	91.7	79.1
	PC2 contribution (%)	20.1	64.0	44.2	8.6	7.8	1.7	1.8	2.4
	Unexplained variability (%)	20.8	15.8	41.7	54.9	50.0	12.9	6.5	18.5
	Measured mean (mg/kg)	3.68	0.16	0.029	24.6	64.8	30.0	21.7	73.3
	Predicted mean (mg/kg)	3.67	0.16	0.031	24.6	64.8	30.0	21.7	73.3
	R <sup>2</sup>	0.81	0.90	0.92	0.73	0.65	0.91	0.90	0.88

Figure 8 illustrates the results of the APCS-MLR method for the source apportionment. The results showed that the concentrations of As, Cr, Cu, Ni, Pb, and Zn in the A horizon were largely influenced by natural sources, with contribution percentages of 81.1%, 69.5%, 76.7%, 66.6%, 49.1%, and 38.8%, respectively. However, the Cd and Hg contents in the A horizon soils were mainly impacted by anthropogenic inputs, corresponding to 50.3% and 57.8%, respectively. In the C horizon soils, natural factors chiefly affected the concentrations of As, Ni, Cu, Zn, Cr, and Pb. The contribution rates were found to be 59.0%, 85.4%, 91.7%, 79.1%, 42.2%, and 36.5%, respectively. In contrast, anthropogenic contributions significantly influenced the Cd and Hg contents in the C horizon’s soil, marking percentages at 64.0% and 44.2%, respectively.

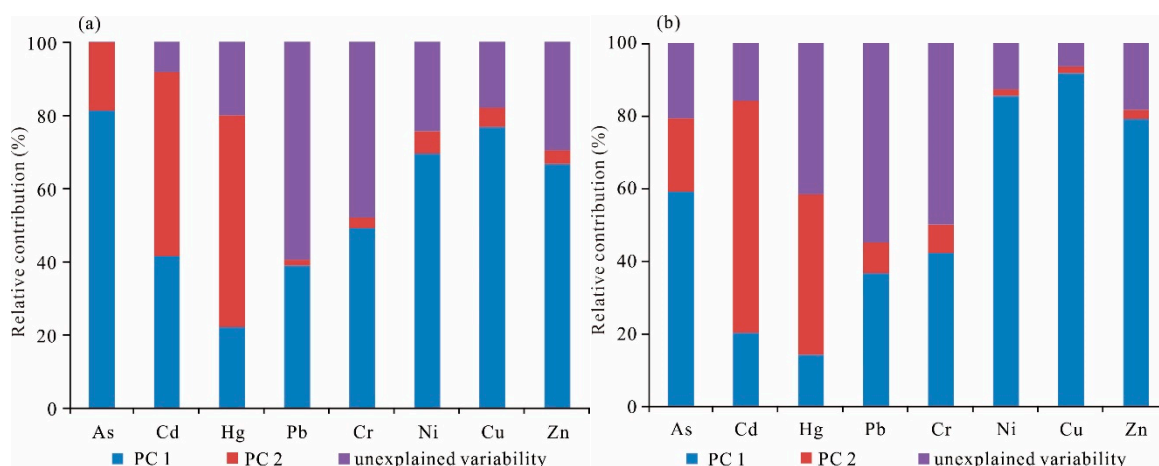


**Figure 8.** Contributions of pollutant sources to A horizon soils (a) and C horizon soils (b) based on the APCS-MLR model.

Compatible origins were noted for heavy metals in both the A and C horizons of the purple soils in the research area. This finding suggested that anthropogenic inputs of Hg and Cd, from coal mining or burning and agriculture have impacted not only the surface soils of the area but also the deeper soils. Furthermore, concerning the proportion of anthropogenic input sources, the percentage of elemental As in the A and C soil horizons also

reached approximately 20% (Figure 8), suggesting that human activities have contributed to the presence of soil As in the study area.

#### 4. Conclusions

In this paper, components from different genetic horizons of purple soil in eastern Guang'an City were analyzed to evaluate the contamination status, ecological hazards, and source apportionment of heavy metals. The main findings of the paper are as follows:

The concentrations of heavy metals in the A horizon of purple soil were higher than those in the C horizon. The average contents of some heavy metals, such as Cd, Cr, Hg, and Ni, exceeded the background values for Chinese purple soil. Strong correlations were found among the heavy metals in the purple soil, except for Cd and Hg. Additionally, the significant correlations between these highly correlated heavy metals and the soil physicochemical properties, such as soil pH, texture, and the contents of Fe and Al, indicated similar geochemical properties or common origins of the heavy metals.

Risk assessment utilizing EF, PLI, and IRI revealed more risk points of heavy metal contamination in the A horizon than in the C horizon. The anomalies were generally related to the contents of Cd and Hg in the soil. The PCA showed that the high loadings of Cd and Hg on PC1 were primarily attributed to anthropogenic sources like coal combustion and agricultural activities. On the contrary, the other heavy metal contents with strong loadings on PC2 mainly originated from natural sources. The APCS-MLR analysis revealed that the levels of Pb and Cr had a high percentage of unidentified contributions, ranging from 48.0% to 59.6%. Anthropogenic sources accounted for 44.2% to 64.0% of the total contributions to the Cd and Hg contents in the A and C horizons, while natural origins accounted for 36.5% to 91.7% of the total contributions to the other heavy metals.

**Author Contributions:** Y.S.: conceptualization, interpretation, and writing the original draft. W.C.: text editing, discussion, supervision, and manuscript review. J.L. and Y.S.: investigation. Y.Z.: resources and software. B.Y.: experimental operation and methodology. H.H.: reviewed the manuscript. All authors have read and agreed to the published version of the manuscript.

**Funding:** This research was sponsored by the Surface Matrix Survey in Guang'an City, Chengdu-Chongqing Economic Circle (DD20220864), and the China Geological Survey Project (DD20243077).

**Data Availability Statement:** The data that support the findings of this study are available from the corresponding author W. C. upon reasonable request.

**Acknowledgments:** The authors gratefully acknowledge D.Z. and J.C. at the Research Center of Applied Geology of the China Geological Survey for their constant help.

**Conflicts of Interest:** The authors declare no conflicts of interest.

#### References

1. Huang, S.S.; Liao, Q.L.; Hua, M.; Wu, X.M.; Bi, K.S.; Yan, C.Y.; Chen, B.; Zhang, X.Y. Survey of heavy metal pollution and assessment of agricultural soil in Yangzhong district, Jiangsu Province, China. *Chemosphere* **2007**, *67*, 2148–2155. [[CrossRef](#)]
2. Chen, L.; Zhou, S.L.; Wu, S.H.; Wang, C.H.; Li, B.J.; Li, Y.; Wang, J.X. Combining emission inventory and isotope ratio analyses for quantitative source apportionment of heavy metals in agricultural soil. *Chemosphere* **2018**, *204*, 140–147. [[CrossRef](#)] [[PubMed](#)]
3. Zeng, J.; Han, G.; Zhang, S.; Liang, B.; Qu, R.; Liu, M.; Liu, J. Potentially toxic elements in cascade dams-influenced river originated from Tibetan Plateau. *Environ. Res.* **2022**, *208*, 112716. [[CrossRef](#)]
4. Lin, H.; Wang, Z.; Liu, C.; Dong, Y. Technologies for removing heavy metal from contaminated soils on farmland: A review. *Chemosphere* **2022**, *305*, 135457. [[CrossRef](#)]
5. Shao, Y.; Yang, Z.; Wang, L.; Zhuo, X.; Zhang, Q. Cadmium bioavailability and influencing factors of soil-rice system in Nanliujiang Catchment of Guangxi. *Geoscience* **2021**, *35*, 625–636. (In Chinese)
6. Wu, G.; Wang, L.; Yang, R.; Hou, W.; Zhang, S.; Guo, X.; Zhao, W. Pollution characteristics and risk assessment of heavy metals in the soil of a construction waste landfill site. *Ecol. Inform.* **2022**, *70*, 101700. [[CrossRef](#)]
7. Rouhani, A.; Bradák, B.; Makki, M.; Ashtiani, B.; Hejman, M. Ecological risk assessment and human health risk exposure of heavy metal pollution in the soil around an open landfill site in a developing country (Khesht, Iran). *Arab. J. Geosci.* **2022**, *15*, 1523. [[CrossRef](#)]
8. Chen, N.; Zheng, Y.; He, X.; Li, X.; Zhang, X. Analysis of the Report on the national general survey of soil contamination. *Nong Ye Huan Jing Ke Xue Xue Bao* **2017**, *36*, 1689–1692. (In Chinese)

9. Liu, Y.; Xiao, T.; Zhu, Z.; Ma, L.; Li, H.; Ning, Z. Geogenic pollution, fractionation and potential risks of Cd and Zn in soils from a mountainous region underlain by black shale. *Sci. Total Environ.* **2021**, *760*, 143426. [[CrossRef](#)]
10. Jalali, M.; Moradi, F.; Jalali, M.; Wang, J. Risk assessment of available and total heavy metals contents in various land use in calcareous soils. *Environ. Earth Sci.* **2023**, *82*, 298. [[CrossRef](#)]
11. Duan, Y.; Yang, Z.; Yu, T.; Yang, Q.; Liu, X.; Ji, W.; Jiang, H.; Zhuo, X.; Wu, T.; Qin, J.; et al. Geogenic cadmium pollution in multi-medians caused by black shales in Luzhai, Guangxi. *Environ. Pollut.* **2020**, *260*, 113905. [[CrossRef](#)] [[PubMed](#)]
12. Bostick, B.C.; Landis, J.D.; Clausen, J.L. Tungsten speciation and solubility in munitions-impacted soils. *Environ. Sci. Technol.* **2018**, *52*, 1045–1053. [[CrossRef](#)] [[PubMed](#)]
13. Zhang, T.; Wang, P.; Wang, M.; Liu, J.; Gong, L.; Xia, S. Spatial distribution, source identification, and risk assessment of heavy metals in riparian soils of the Tibetan plateau. *Environ. Res.* **2023**, *237*, 116977. [[CrossRef](#)]
14. Pan, P.; Yang, J.; Deng, S.; Jiang, H.; Zhang, J.; Li, L.; Shen, F. Proceedings and prospects of pesticides and heavy metals contamination in soil-plant system. *Nong Ye Huan Jing Ke Xue Xue Bao* **2011**, *30*, 2389–2398. (In Chinese)
15. Wen, Y.; Li, W.; Yang, Z.; Zhang, Q.; Ji, J. Enrichment and source identification of Cd and other heavy metals in soils with high geochemical background in the karst region, Southwestern China. *Chemosphere* **2020**, *245*, 125620. [[CrossRef](#)] [[PubMed](#)]
16. Qu, M.; Li, W.; Zhang, C.; Huang, B.; Hu, W. Source apportionment of soil heavy metal Cd based on the combination of receptor model and geostatistics. *Zhongguo Huanjing Kexue* **2013**, *33*, 854–860. (In Chinese)
17. Sun, L.; Guo, D.K.; Liu, K.; Meng, H.; Zheng, Y.J.; Yuan, F.Q.; Zhu, G.H. Levels, sources, and spatial distribution of heavy metals in soils from a typical coal industrial city of Tangshan, China. *CATENA* **2019**, *175*, 101–109. [[CrossRef](#)]
18. Wang, S.; Cai, L.M.; Wen, H.H.; Luo, J.; Wang, Q.S.; Liu, X. Spatial distribution and source apportionment of heavy metals in soil from a typical county-level city of Guangdong Province, China. *Sci. Total Environ.* **2019**, *655*, 92–101. [[CrossRef](#)] [[PubMed](#)]
19. Thurston, G.D.; Spengler, J.D. A quantitative assessment of source contributions to inhalable particulate matter pollution in metropolitan Boston. *Atmos. Environ.* **1985**, *19*, 9–25. [[CrossRef](#)]
20. Tapper, U.; Paatero, P. Positive matrix factorization: A non-negative factor model with optimal utilization of error estimates of data values. *Environmetrics* **1994**, *5*, 111.
21. Zhang, J.; Xia, J.; Chen, S.; Wu, Y.; Pang, Y.; Huang, T. Source analysis of heavy metal lead in Luoma Lake sediments based on Pb stable isotopes. *J. Environ. Eng. Technol.* **2023**, *13*, 1011–1020. (In Chinese)
22. Lv, J.S. Multivariate receptor models and robust geostatistics to estimate source apportionment of heavy metals in soils. *Environ. Pollut.* **2019**, *244*, 72–83. [[CrossRef](#)]
23. Zhang, H.; Cheng, S.; Li, H.; Fu, K.; Xu, Y. Groundwater pollution source identification and apportionment using PMF and PCA-APCA-MLR receptor models in a typical mixed land-use area in Southwestern China. *Sci. Total Environ.* **2020**, *741*, 140383. [[CrossRef](#)]
24. Zhang, T.; Wang, M.; Bai, G.; Liu, J.; Li, P.; Zhang, Y.; Xia, S. Distribution characteristics, risk assessment, and source analysis of heavy metals in surface sediments and near-lakeshore soils of a plateau lake in China. *Gondwana Res.* **2023**, *115*, 191–200. [[CrossRef](#)]
25. Zhang, W.; Yan, Y.; Yu, R.; Hu, G. The sources-specific health risk assessment combined with APCS/MLR model for heavy metals in tea garden soils from south Fujian Province, China. *CATENA* **2021**, *203*, 105306. [[CrossRef](#)]
26. Pan, Z.; Peng, H. Comparative study on the global distribution and geomorphic development of red beds. *Sci. Geol. Sin.* **2015**, *35*, 1575–1584. (In Chinese)
27. Meng, Q.; Li, S.; Liu, B.; Hu, J.; Liu, J.; Chen, Y.; Ci, E. Appraisal of soil taxonomy and the world reference base for soil resources applied to classify purple soils from the Eastern Sichuan Basin, China. *Agronomy* **2023**, *13*, 1837. [[CrossRef](#)]
28. Zhong, S.; Han, Z.; Du, J.; Ci, E.; Ni, J.; Xie, D.; Wei, C. Relationships between the lithology of purple rocks and the pedogenesis of purple soils in the Sichuan Basin, China. *Sci. Rep.* **2019**, *9*, 13272. [[CrossRef](#)] [[PubMed](#)]
29. Zhu, X.Y.; Zhu, B. Diversity and abundance of soil fauna as influenced by long-term fertilization in cropland of purple soil, China. *Soil Till. Res.* **2015**, *146*, 39–46. [[CrossRef](#)]
30. Li, Z.; Wang, P.; Liu, L.; Zheng, Y.; Xie, D. High negative surface charge increases the acidification risk of purple soil in China. *CATENA* **2021**, *196*, 104819. [[CrossRef](#)]
31. Wei, F.; Chen, J.; Wu, Y.; Zheng, C. Study on background values of soil environment in China. *Huanjing Kexue* **1991**, *4*, 12–19. (In Chinese)
32. Li, Y.; Zhang, W.; Cheng, Y.; Li, Z.; Xie, D. Environmental geochemical baseline of As and Hg in purple soil and its parent rock in Chongqing. *Acta Pedol. Sin.* **2017**, *54*, 917–926. (In Chinese)
33. Wu, F.; Chen, L.; Yi, T.; Yang, Z.; Chen, Y. Determination of heavy metal baseline values and analysis of its accumulation characteristics in agricultural land in Chongqing. *Huanjing Kexue* **2018**, *39*, 5116–5126. (In Chinese) [[PubMed](#)]
34. Zheng, S.; Zheng, X.; Zhang, T.; Liu, S. Study on leaching characteristics and release kinetics of heavy metals in polluted purple soil. *J. Soil Water Conserv.* **2011**, *25*, 253–256. (In Chinese)
35. Li, Q.; Zhao, X. Enrichment characteristics of heavy metals in particulate organic matter of purple paddy soil. *Huanjing Kexue* **2017**, *38*, 2146–2153. (In Chinese) [[PubMed](#)]
36. Du, J.; Wang, Z.; Liu, J.; Zhong, S.; Wei, C. Distribution characteristics of soil heavy metals, their source identification and their changes influenced by anthropogenic cultivation activities in purple hilly regions of Sichuan Basin, China. *J. Soil Sci. Plant Nutr.* **2020**, *20*, 1080–1091. [[CrossRef](#)]

37. Liu, C.; Qin, Y.; Zhao, X. Long-term effect of fertilization on accumulation and availability of heavy metal in a calcareous paddy soil. *Nong Ye Huan Jing Ke Xue Xue Bao* **2020**, *39*, 1494–1502. (In Chinese)
38. Wang, L.; Zou, Y.; Wei, Z.; Cai, Y. The Xujiahe Formation coal measures in Guang'an Area, Sichuan Basin. *Nat. Gas Geosci.* **2012**, *23*, 153–160. (In Chinese)
39. Guang'an Yearbook Compilation Committee. *Guang'an Yearbook*; China Business Association Press: Guang'an, China, 2022. (In Chinese)
40. Zhao, X.; Yang, Z.; Cheng, H.; Ma, X.; Wang, J.; Li, Z.; Wang, C.; Li, M.; Lei, F. Geochemical characteristics and ecological health-related ranges of Copper in soil in Huaying Mountain-Xicao in Linshui County, Sichuan Province. *Geophys. Geochem. Explor.* **2022**, *46*, 238–249. (In Chinese)
41. Feng, C. Geochemical Characterization of Soil Cadmium in Western Guangxi County, Guang'an, Sichuan, China. Master's Thesis, China University of Geosciences (Beijing), Beijing, China, 2021. (In Chinese).
42. Zhang, G.; Li, D. *Field Soil Description and Sampling Manual*; Science Press: Beijing, China, 2022. (In Chinese)
43. Lv, Y.; Li, B. *Soil Science*; China Agriculture Press: Beijing, China, 2019. (In Chinese)
44. Chester, R.; Stoner, J.H. Pb in Particulates from the Lower Atmosphere of the Eastern Atlantic. *Nature* **1973**, *245*, 27–28. [[CrossRef](#)]
45. Qi, C.; Xu, M.; Liu, J.; Li, C.; Yang, B.; Jin, Z.; Liang, S.; Guo, B. Source analysis and contribution estimation of heavy metal contamination in agricultural soils in an industrial town in the Yangtze River Delta, China. *Minerals* **2024**, *14*, 279. [[CrossRef](#)]
46. Huang, X.; Han, P.; Ma, M.; Cao, Q.; Li, W.; Wan, F.; Zhang, X.; Chai, Q.; Zhong, L.; Li, B. Investigating the source apportionment of heavy metals in soil surrounding reservoir using partial least-squares regression model. *Water Supply* **2022**, *22*, 3908–3920. [[CrossRef](#)]
47. Ding, X.; Ye, S.; Laws, E.A.; Mozdzer, T.J.; Yuan, H.; Zhao, G.; Yang, S.; He, L.; Wang, J. The concentration distribution and pollution assessment of heavy metals in surface sediments of the Bohai Bay, China. *Mar. Pollut. Bull.* **2019**, *149*, 110497. [[CrossRef](#)]
48. Hakanson, L. An ecological risk index for aquatic pollution control. a sedimentological approach. *Water Res.* **1980**, *14*, 975–1001. [[CrossRef](#)]
49. Sutherland, R.A. Bed sediment-associated trace metals in an urban stream, Oahu, Hawaii. *Environ. Geol.* **2000**, *39*, 611–627. [[CrossRef](#)]
50. Shao, Y.; Yan, B.; Liu, L.; Yu, X.; Feng, G.; Zhang, K.; Gong, K. Hydrochemical characteristics and quality evaluation of irrigation and drinking water in Bangong Co Lake watershed in Northwest Tibetan Plateau. *Water* **2023**, *15*, 2655. [[CrossRef](#)]
51. Zhao, B.; Zhu, W.; Hao, S.; Hua, M.; Liao, Q.; Jing, Y.; Liu, L.; Gu, X. Prediction heavy metals accumulation risk in rice using machine learning and mapping pollution risk. *J. Hazard.* **2023**, *448*, 130879. [[CrossRef](#)]
52. Lin, Z.; Huang, Z.; Liao, D.; Huang, W.; Huang, J.; Deng, Y. Effects of soil organic matter components and iron aluminum oxides on aggregate stability during vegetation succession in granite red soil eroded areas. *J. Mt. Sci.* **2022**, *19*, 2634–2650. [[CrossRef](#)]
53. Wedepohl, K.H. Ingerson lecture the composition of the continental crust. *Geochim. Cosmochim. Acta* **1995**, *59*, 1217–1232. [[CrossRef](#)]
54. Wu, K.; Zhao, R. Soil texture classification and its application in China. *Acta Pedol. Sin.* **2019**, *56*, 227–241. (In Chinese)
55. Wang, Y. Study on the Development Processes of Rill Erosion in Purple Soil Region. Master's Thesis, Sichuan Agricultural University, Chengdu, China, 2019. (In Chinese).
56. Reis, A.T.; Davidson, C.M.; Vale, C. Overview and challenges of mercury fractionation and speciation in soils. *TrAC-Trend Anal. Chem.* **2016**, *82*, 109–117. [[CrossRef](#)]
57. Ruan, X.; Ge, S.; Jiao, Z.; Zhan, W.; Wang, Y. Bioaccumulation and risk assessment of potential toxic elements in the soil-vegetable system as influenced by historical wastewater irrigation. *Agric. Water Manag.* **2023**, *279*, 108197. [[CrossRef](#)]
58. Chen, M.; Kong, Y.; Zheng, W.; Liu, J.; Wang, Y.; Wang, Y. Accumulation and risk assessment of mercury in soil as influenced by mercury mining/smelting in Tongren, Southwest China. *Environ. Geochem.* **2024**, *46*, 83. [[CrossRef](#)]
59. Wen, Y.; Wang, Y.; Ji, W.; Wei, N.; Liao, Q.; Huang, D.; Meng, X.; Song, Y. Influencing factors of elevated levels of potentially toxic elements in agricultural soils from typical karst regions of China. *Agronomy* **2023**, *13*, 2230. [[CrossRef](#)]
60. Morel, F.M.M.; Kraepiel, A.M.L.; Amyot, M. The chemical cycle and bioaccumulation of mercury. *Annu. Rev. Ecol. Syst.* **1998**, *29*, 543–566. [[CrossRef](#)]
61. Hingorani, R.; Jiménez-Relinque, E.; Grande, M.; Castillo, Á.; Nevshupa, R.; Orcid, C.; Castellote, M. From analysis to decision: Revision of a multifactorial model for the in situ assessment of NOx abatement effectiveness of photocatalytic pavements. *Chem. Eng. J.* **2020**, *402*, 126250. [[CrossRef](#)]

**Disclaimer/Publisher's Note:** The statements, opinions and data contained in all publications are solely those of the individual author(s) and contributor(s) and not of MDPI and/or the editor(s). MDPI and/or the editor(s) disclaim responsibility for any injury to people or property resulting from any ideas, methods, instructions or products referred to in the content.